ISSN 0027-1349, Moscow University Physics Bulletin, 2007, Vol. 62, No. 4, pp. 260–265. © Allerton Press, Inc., 2007.
Original Russian Text © V.I. Zakharov, V.E. Kunitsyn, 2007, published in Vestnik Moskovskogo Universiteta. Fizika, 2007, No. 4, pp. 69–74.

Possibilities of Radio Occultation Sounding Using the GPS/GLONASS System for Regional Monitoring of the Atmosphere

V. I. Zakharov and V. E. Kunitsyn

Department of Physics of the Atmosphere, Faculty of Physics, Moscow State University, Leninskie gory, Moscow, 119992 Russia

e-mail: atm5571@phys.msu.su

Received October 11, 2006

Abstract—The possibilities of retrieving the parameters of atmospheric structures from radio-occultation sounding data are discussed using the examples of a cyclone and an atmospheric front with different parameters. It is shown that the reconstructed images of such structures are highly distorted (up to tens of percents) and often contain artifacts, both factors complicating the interpretation of meteorological data obtained in radio-occultation experiments.

DOI: 10.3103/S0027134907040133

INTRODUCTION

Methods providing reliable on-line information on atmospheric processes appearing and evolving on different scales and on current weather conditions are necessary both for synoptic forecasting and for solving a number of geophysical problems, including interactions between geospheres. Of wide use for this purpose are the methods of remote monitoring and, particularly, radio sounding, with its comprehensive theoretical basis and well-developed measurement technique.

In the recent decade, methods used for remote monitoring are closely associated with radio occultation (RO) sounding and refractometry (RM). After the success of the experiments at the MIR station and the GPS/MET, CHAMPION, and Orsted satellites, these methods have passed into the ranks of conventional practice. The data provided by these methods are used in meteorological research, for verification of climate models, etc. Along with this, the RO sounding method faces a number of problems due to inhomogeneous structures, whose presence in the propagation media affects the reconstruction accuracy.

The future development of RO sounding methods—associated with the creation of application-specific small satellites for atmospheric and ionospheric studies—will inevitably encounter limitations imposed by the method for gaining the primary information. Therefore, it seems important to take a closer look at the possible errors in the reconstruction and interpretation of RO data. The aim of this study is to model and analyze the effects of inhomogeneous structures on the accuracy of reconstructing atmospheric parameters in various conditions. Unlike an in situ experiment, a model experiment allows the influences of different sources to be estimated. The reconstruction features specific for different atmospheric structures are analyzed.

1. RADIO-OCCULTATION SOUNDING OF THE ATMOSPHERE

Radio-occultation sounding has long been known [1, 2] and is advantageously used today to investigate the atmospheres of planets (a vast bibliography on this subject can be found in [3]). The method can be generalized for the case of sounding the ionosphere of planets, including the Earth [3–7]. In the principal scheme of an RO experiment, a satellite observes the radio rise (set) of another satellite bearing a source of electromagnetic waves. As the satellites move, different cross sections of the media are probed and the ionosphere and atmosphere can be sounded separately. The GPS system operating frequencies used in such studies were 1575.42 MHz (f_1 or $L1$) and 1227.6 MHz (f_2 or $L2$).

In case of a layered system, the vertical profile of the refractive index $n(h)$ is related to the vertical profile of the refraction angle via the Abelian transform [1, 2]. The reconstructed profile is recast into the profiles of meteorological parameters. The vertical RO resolution is determined by the size of the first Fresnel zone and amounts to hundreds of meters for the decimeter band in the Earth's atmosphere. Horizontal resolution in the plane of sounding is determined by the path length of beam L_a in a layer of thickness equal to the homogeneous atmosphere height H_0: $L_a = \sqrt{2H_0R}$ (where $H_0 \ll R$), which yields $L_a = 400$–600 km for the Earth's radius $R \approx 6400$ km and $H_0 \approx 5$–10 km.

Of most interest in the Earth's atmosphere and ionosphere are variations of their parameters, such as temperature, pressure, and humidity. These parameters should be determined to a high accuracy [3–8], which has only been attained in the last 15 years. According to available commercial data [5–7] and a number of estimates [9–13], the effect of the propagation media on the accuracy of reconstructed meteorological parameters is comparable to, and sometimes even more than, the effect of instrumentation errors. Perturbation dynamics and multibeam propagation that take place in particular cases [10, 14], as well as ionospheric influence [4, 9] superimpose on atmosphere variations and additionally complicate the interpretation of data.

2. MODELING OF RADIO-OCCULTATION EXPERIMENTS

The modeling of RO experiments is based on solving equations for wave propagation in near-earth space and finding the signal parameters that can be verified in experiments: amplitude, phase, group delay, Doppler shift, and refraction angle, as functions of the target parameter [8–12]. As a result of modeling, the dynamics of signal propagation can be described with allowance for inhomogeneous structures, the self-effect of the media [9], multibeam propagation [10, 14], and effects on caustic surfaces, i.e., the limitations of geometric optics [13, 14, 15]. Nonetheless, the ray approximation is widely used in the simulation of RO experiments because it adequately describes the main features of signal propagation.

Similarly to [12, 13], we used a 3D model of the medium and considered the propagation of signal in the approximation of geometric optics. This statement of problem has a number of complications as compared with the 2D statement. One difficulty is that of obtaining smooth fields of meteorological parameters and their first derivatives given a discrete sampling in the nodes of the model (see [12, 13]).

Profiles of the spatial refraction index $n(\mathbf{r})$ were modeled similarly to [8–11] but for the 3D case,

$$n(\mathbf{r}) = 1 + 10^{-6}[N_{\text{atm}}(\mathbf{r}) + \delta N_{\text{atm}}(\mathbf{r}, \ldots) - (f_c^2/f^2)(N_e(\mathbf{r}) + \delta N_e(\mathbf{r}, \ldots))/N_{e_{\max}}(\mathbf{r})], \quad (1)$$

where the altitude profile of the regular refraction of the atmosphere, $N_{\text{atm}}(\mathbf{r})$, is taken in the form of the exponential profile of the International Committee on Radio Frequencies, $N_e(\mathbf{r}, \ldots)$ is the electron concentration in the ionosphere (a set of parabolic layers), ellipses in the arguments denote the position and parameters of inhomogeneous structures, f_c is the critical frequency, $N_{e_{\max}}$ is the electron concentration at the maximum level, and δ denotes variation of a parameter.

Inhomogeneous structures were modeled by various functions additive to (1) (see [8–11]). For example, it has been proposed [8, 11] that the refractive index of the atmospheric front in the cross section along the direction of sounding can be taken in the form

$$n(h, \theta) = N_{\text{atm}}(h)G(h)[1 + \beta F(\xi)], \quad (2)$$

where F is a function of type erf(ξ), $\xi \subset [-\infty, +\infty]$, or $\cos^2(\pi\xi/2)$, $\xi \subset [0, 1]$ and $\xi = [\theta - \theta_0 + (h/\gamma L_f)]/\Delta\theta$, and β is the intensity (amplitude) of the wave front. Coordinates (h, θ) are specified in the section of the wave front by the sounding plane. The parameters have a clear physical meaning: h is the altitude of localization of the perturbation, L_f is the front length, and γ is the tangent of the angle between the wave front and the Earth surface. The function $G(h) = \exp(-\gamma h/H_{\text{atm}})$ describes a decrease in the perturbation with altitude, and parameters $\gamma \subset [0, \ldots, 5]$ are chosen to comply with the experiment.

Modeling of both the direct and inverse problems is known as 'end-to-end' modeling. The spatial step is chosen to be 100 m in the atmosphere and approximately 1 km in the ionosphere ($h > 60$ km). The accuracy of solving the direct problem is largely determined by the accuracy of positioning the satellites and is better than 10^{-12} in terms of the orientation angle; in the case of a spherically symmetric medium, this leads to less than a 0.1% error in the reconstructed profiles of meteorological parameters.

The influence of the ionosphere on the atmospheric profile was compensated using the double-frequency method [4]. For a real ionosphere containing inhomogeneities, the compensation quality may deteriorate. As a result, artifacts may appear in the atmospheric profiles, as was predicted in [9] and experimentally supported in [12]. The profile $n(\mathbf{r})$ was reconstructed using the Abelian transform [1, 2], $n(\mathbf{r})$ was assigned to the perigee points of the sounding rays.

Among the methods elaborated for RO data analysis are the 4D-Var approach [13] related to the method of direct variation assimilation of data [17] and the method of nonlinear estimation [16]. These methods rely on the information obtained in different models and measurements, i.e., they take the atmospheric dynamics into account. The comparison of these methods with real situations reveals a number of additional problems, which lie beyond the scope of the present study.

3. DISCUSSION OF THE MODEL RESULTS

In the course of the numerical experiment (see section 2) we considered typical variants of a horizontally inhomogeneous atmosphere with perturbations measuring from hundreds to thousands of kilometers. In many cases, the reconstructions miss some features of the preset models and structures smaller than 400 km are heavily distorted. The larger structures resemble the original shape but the local profiles can be distorted significantly.

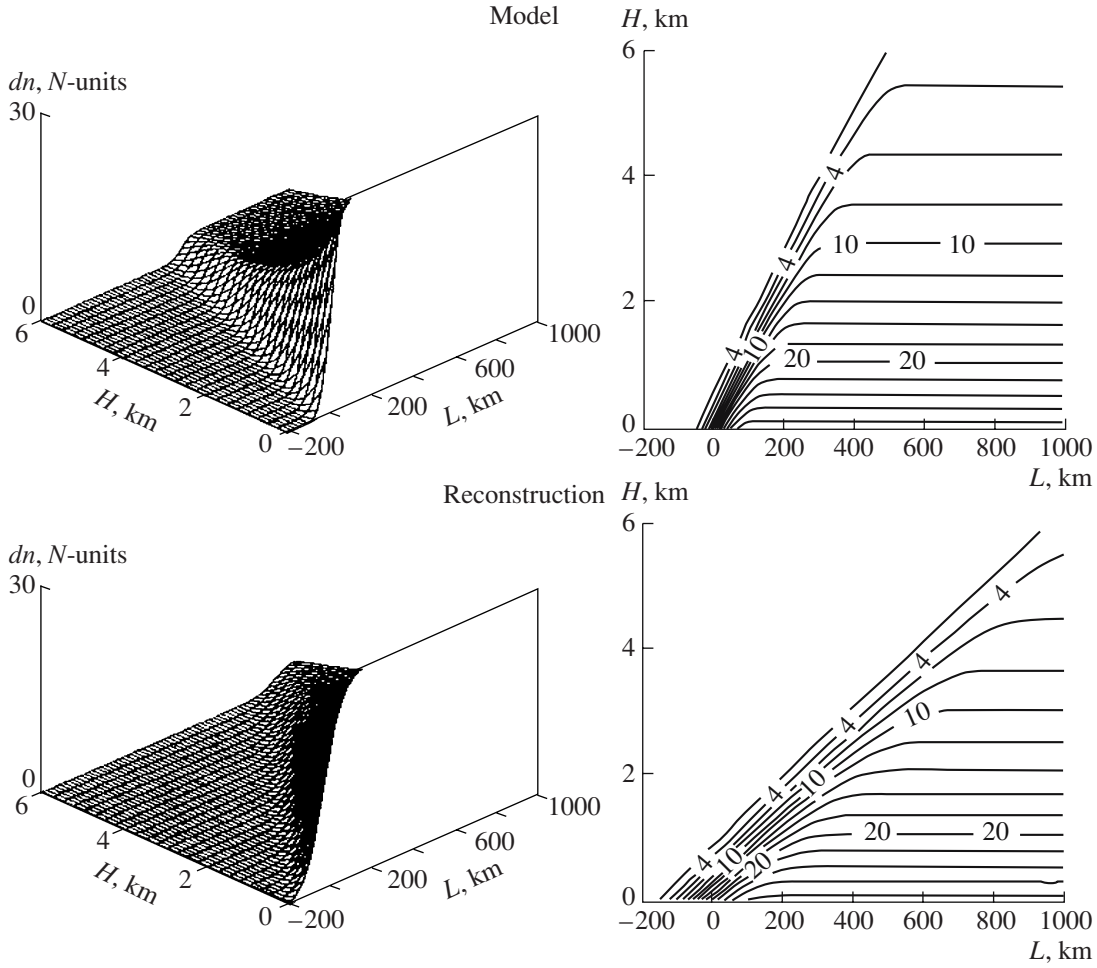

Fig. 1. Radio-occultation sounding of an atmospheric front.

The presence of atmospheric structures breaks the quasi-spherical symmetry of the problem, since the information about them will be contained in the reconstruction, even if a part of such a structure falls into the sounding range with a typical atmospheric size of L_a. Consider a mental RO experiment, in which sounding signal is transmitted between two low-orbit satellites moving along the same orbit with a radius of 800 km over the Earth's surface one after the other, such that the perigee points of the sounding rays are spaced by a distance of 10 km in the projection onto the Earth's surface. The set of profiles reconstructed in a large number of numerical experiments (from 100 to 240) forms a surface, which should be compared with the original model. Below, such surfaces summarizing the results of numerical experiments are considered in more detail. Cross sections L = const correspond to a profile obtained in a particular RO experiment. To avoid overcomplicating the pattern, regular dependences $n(h)$ are omitted.

3.1. The results obtained indicate that the atmospheric front in the RO experiments is smeared in the horizontal direction. Reconstructions of smooth fronts, for which the tangent of the surface inclination angle $|\gamma| < 0.02$ (see (2)), are close to the originals, but reconstructions of steep meteorological fronts (of width L_f = 50–100 km) display significant distortions (see Fig. 1). The top panel in Fig. 1 plots the model atmospheric front and the bottom shows the set of all possible reconstructions with L_f = 50 km, H = 3 km, α = 3, and γ = 0.05 (see (2)). The inclination angle of the retrieved front decreases by a factor of L_a/L_f. The reconstruction errors depend on the amplitude and size of the perturbation and can typically be as high as 1–10% depending on the front parameters. Figure 2 presents the topology of relative reconstruction errors $\delta = (1 - n_{\text{ret}}(r)/n_{\text{mod}}(r)) \times 100\%$ for the front with parameters specified above. The ultimate inclination angle of the wave front is on the order of the regular refraction in the atmosphere, which is about 20 mrad in the case of the Earth.

3.2. The capabilities of the RO sounding method for atmospheric monitoring were also considered using the example of cyclones. To describe this type of perturbation, the regular profile of the refractive index (1) was superposed with an ellipsoid of rotation with a narrow inside notch simulating the cyclone's eye.

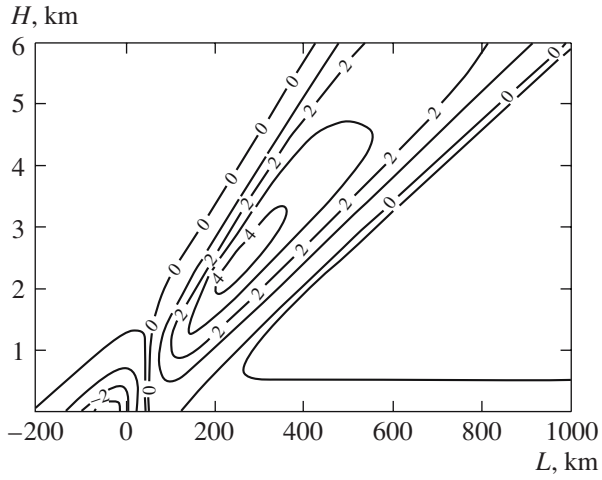

Fig. 2.

The calculation was carried out using the data for the well-known hurricane Katrina (August 23–30, 2005) at the period when it was rated as a 4–5 category hurricane. According to space images, Katrina evolved from hundreds to 1200 km in diameter with its eye (the central region clear from clouds in the optical range) measuring about 100–300 km in diameter. For modeling, the cyclone sizes were taken to be 200, 600, and 1200 km.

Perturbations of $n(h)$ due to cyclone propagation were estimated on the basis of meteorological data such as temperature, pressure, and precipitation measured along the propagation path [19–21]. The literature data suggest that perturbation of the refractive index due to a category 4–5 cyclone is about 30–50 N units, i.e., 10–15% of its regular value.

In many cases, the profiles retrieved by the RO method did not contain the features that were present in the initial models. Figure 3 shows the reconstruction of the model cyclone at two different evolution stages

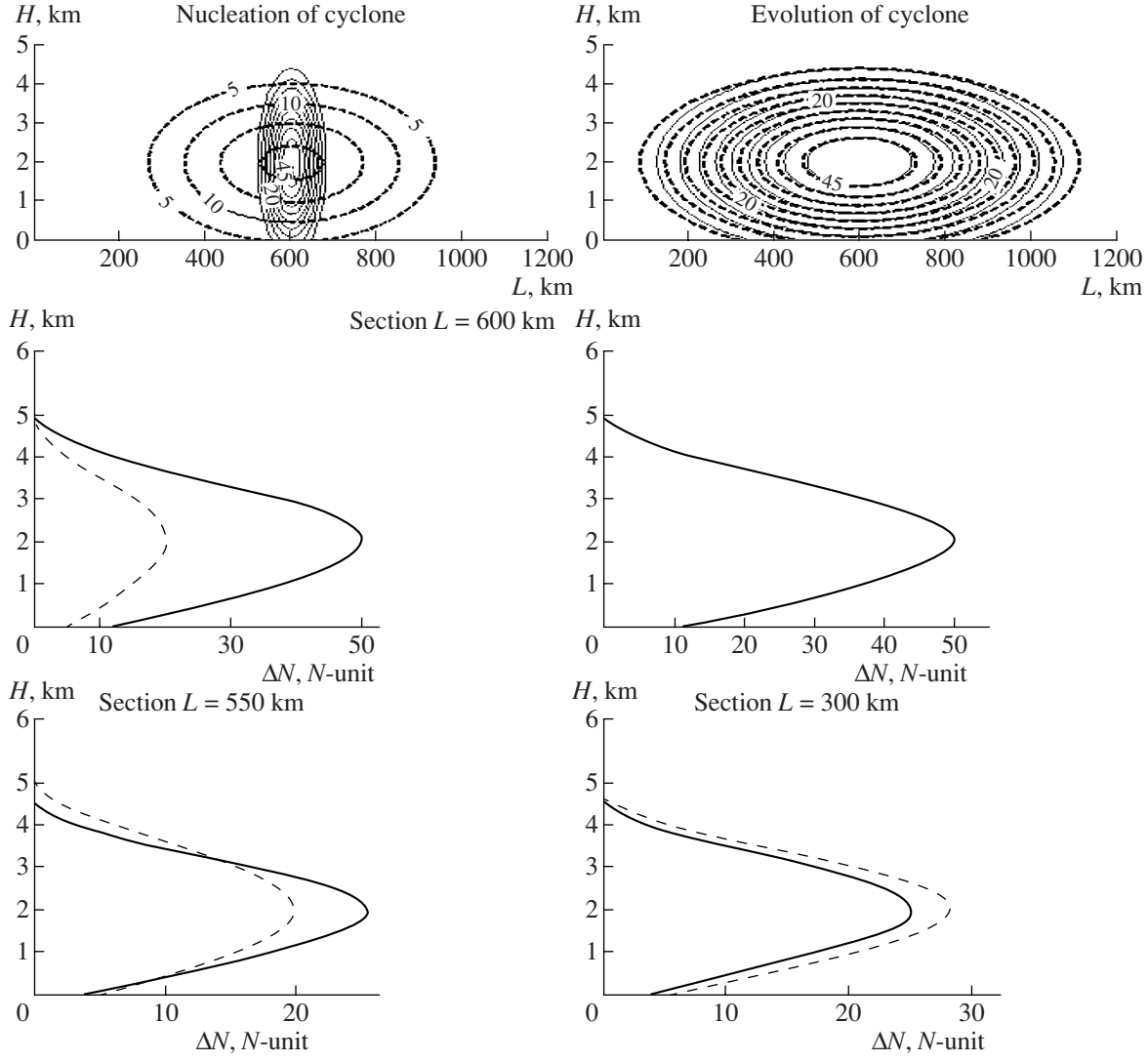

Fig. 3. Reconstruction (solid line) of a model (dashed line) of a cyclone at different stages of its development.

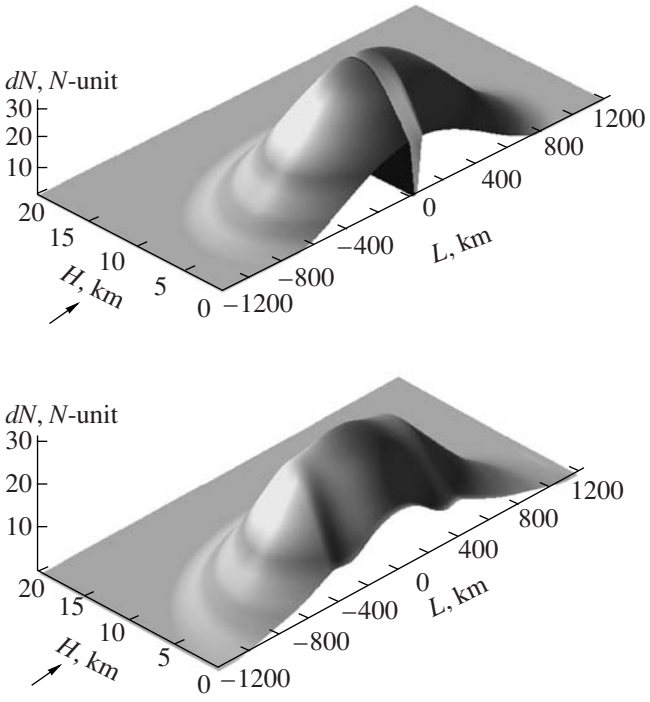

Fig. 4. Altitude distribution of an atmospheric perturbation in the form of a developed cyclone with an eye: model (top) and reconstruction from the RO experiment (bottom). Arrow marks the sounding direction (satellite-to-satellite line of sight).

characterized by the cyclone length of 200 and 1200 km along the Earth's surface. Both structures have the same thickness of 4 km, equal intensity of 50 N units, and are localized at an altitude of 2 km over the Earth's surface.

The left panel of Fig. 3 illustrates the reconstruction of a 200 km long structure. Such structures are evidently distorted by the RO sounding method. The altitude sections of the model and retrieved profiles are compared at the bottom of the same panel. It is seen that the discrepancies reach 70% in the section passing through the model maximum ($L = 600$ km) and 15% in section $L = 550$ km, the most "successful" section. The region $L \subset [200–500]$ km contains artifacts, i.e., it displays a structure that was not actually there.

The situation is much better with the perturbation of length 1200 km. In particular, the section $L = 600$ km is retrieved with an accuracy better than 1% (see the middle plot of the right panel). The discrepancy begins to grow toward the periphery of the structure and is 12% in the section $L = 300$ km. Note that the altitude position of the perturbation maximum is exactly defined in all the cases.

3.3. The analysis shows that the reconstruction accuracy depends on the perturbation sign, i.e., on whether the inhomogeneous structure protrudes over the average level. This thesis is illustrated by Fig. 4, which shows the model (top) and reconstruction (bottom) of a cyclone with a 150-km-wide eye. In the eye of the model cyclone, the perturbation amplitude drops

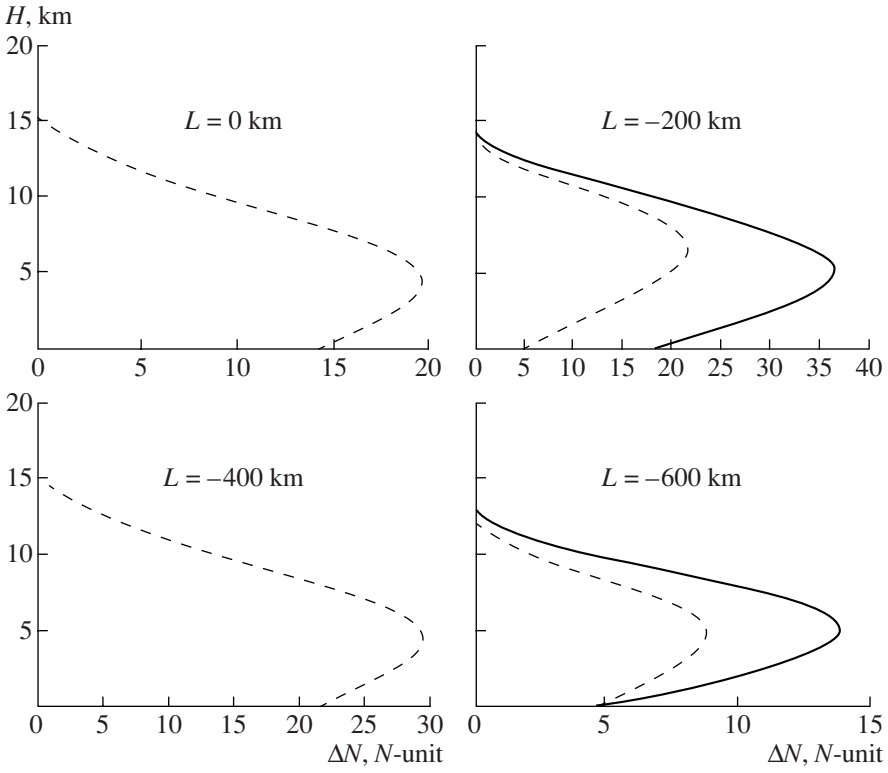

Fig. 5. Typical errors and artifacts arising in the retrieved profiles (dashed line) for the model (solid line) in Fig. 4.

to zero, i.e., its sign is opposite to that of the cyclone body. Other parameters of the structure are presented above. It is seen that the reconstruction of the small-size eye fails and the gradient of the refraction index at the eye boundaries gives rise to quasi-perturbations at the region $L = \pm 400$ km. Figure 5 indicates that, at $L = 0$ km, the retrieved profile contains artifacts; at $L = -200$ km, the discrepancies reach 30%; at $L = -400$ km, the errors change sign; and at $L = -600$ km, the errors exceed 40%.

The examples considered above illustrate the difficulty of independent interpretation of RO sounding data. Indeed, any of the profiles shown in Figs. 3–6 can be realized in a particular RO experiment, since neither the orientation of the inhomogeneous structures nor their location, type, and even the sign of the perturbation $n(h)$ are known beforehand.

CONCLUSIONS

The radio-occultation sounding method allows the reconstruction of profiles of meteorological parameters with an accuracy sufficient for practical applications if the atmospheric structures are rather large (exceed 600 km). In the case of small (less than 300–400 km) or complicated atmospheric structures (for example, a developed cyclone with an eye), reconstruction errors substantially increase. For steep fronts of pressure, the inclination angle of the front surface changes and artifacts may appear in the retrieved profile. The number of errors also depends on the sign of the perturbation in the inhomogeneous structure.

The presence of a local atmospheric inhomogeneity inevitably complicates the interpretation of a particular RO profile, since the reconstruction result depends on the inhomogeneity position with respect to the perigee point of the sounding rays and cannot be interpreted unambiguously.

Summarizing the results of the study, it should be noted that RO sounding is effective for large-scale atmospheric structures. However, the locally unnormalized errors arising in the presence of perturbations make it difficult to interpret the data obtained using only the RO method. To improve the accuracy of meteorological parameters to the level demanded by applications and to adequately interpret RO data will require a complex approach to the diagnostics of all the probed media and the integration of data obtained by different methods combining space- and land-based monitoring and including the atmosphere tomography.

ACKNOWLEDGMENTS

This study was supported in part by the Russian Foundation for Basic Research, project nos. 06-05-64988a and 05-05-65145a.

REFERENCES

1. R. A. Phinney and D. L. Anderson, J. Geophys. Res. **73** (5), 1819 (1968).
2. V. I. Tatarskii, Izv. Akad. Nauk SSSR, Fiz. Atmos. Okeana **4** (8), 811 (1968).
3. O. I. Yakovlev, *Space Radio Physics* (RFFI, Moscow, 1998) [in Russian].
4. V. V. Vorob'ev and T. G. Krasil'nikova, Izv. Ross. Akad. Nauk, Ser. Fiz. **29** (5), 626 (1993).
5. E. R. Kursinski, G. A. Hajj, W. I. Bertiger, et al., Science **271** (5252), 1107 (1996).
6. R. Ware, M. Exner, D. Feng, et al., Bull. Am. Meteorol. Soc. **77** (1), 19 (1996).
7. *Earth Observation with CHAMP. Results from Three Years in Orbit*, Ed. by C. Reigberg, H. Luhr, P. Schwintzer, and J. Wickert (Springer, 2005).
8. A. S. Gurvich and S. V. Sokolovskii, Izv. Akad. Nauk SSSR, Fiz. Atmos. Okeana **21** (1), 12 (1988).
9. V. I. Zakharov and V. E. Kunitsyn, Vestn. Mosk. Univ., Ser. 3: Fiz., Astron., No. 4, 45 (1998).
10. V. I. Zakharov and V. E. Kunitsyn, Vestn. Mosk. Univ., Ser. 3: Fiz., Astron., No. 4, 46 (1999).
11. V. E. Kunitsyn, V. I. Zakharov, N. A. Berbeneva, et al., Phys. Chem. Earth A **26** (3), 131 (2001).
12. V. Kunitsyn, V. Zakharov, K. Dethloff, et al., Phys. Chem. Earth **29**, 277 (2004).
13. X. Zou, F. Vandenberghe, B. Wang, et al., J. Geophys. Res. D **104**, 22301 (1999).
14. M. E. Gorbunov, *Danish Meteorological Institute, Technical Report 01-02* (DMI, 2001).
15. M. E. Gorbunov and A. S. Gurvich, Radio Sci. **35** (4), 1025 (2000).
16. B. R. Bean and E. J. Dutton, *Radio Meteorology* (Dover, New York, 1968).
17. M. E. Gorbunov and L. Kornbluech, *Max Planck Inst. for Meteorology* (Hamburg, 2003), no. 30, p. 34.
18. P. I. Palmer, J. J. Barnett, J. R. Eyre, et al., J. Geophys. Res. **105**, 17513 (2000).
19. http://www.wunderground.com/hurricane/hurrarchive.asp
20. http://www.msnbc.msn.com/id/3033055/; http://www.msnbc.msn.com/id/7845030/
21. http://earthobservatory.nasa.gov/Newsroom/NewImages/images.php